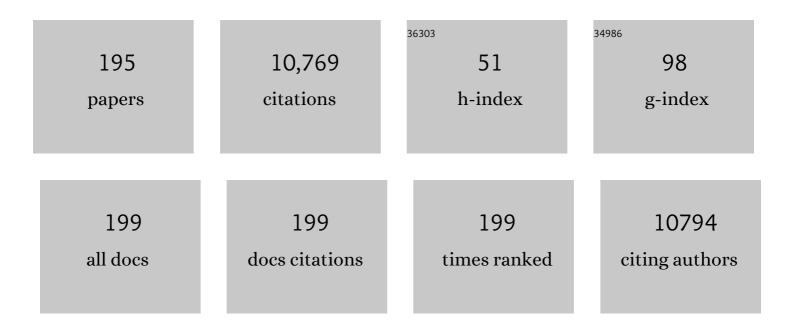
List of Publications by Year in descending order

Source: https://exaly.com/author-pdf/3514067/publications.pdf Version: 2024-02-01



#	Article	IF	CITATIONS
1	Effects of Bi-dopant and co-catalysts upon hole surface trapping on La2Ti2O7 nanosheet photocatalysts in overall solar water splitting. Nano Research, 2022, 15, 438-445.	10.4	16
2	Single-molecule Fluorescence Kinetic Sandwich Assay Using a DNA Sequencer. Chemistry Letters, 2022, 51, 139-141.	1.3	1
3	Enhanced Photocatalytic Activity of Porphyrin Nanodisks Prepared by Exfoliation of Metalloporphyrin-Based Covalent Organic Frameworks. ACS Omega, 2022, 7, 7172-7178.	3.5	13
4	Fluorescein-Based Type I Supramolecular Photosensitizer via Induction of Charge Separation by Self-Assembly. Jacs Au, 2022, 2, 1472-1478.	7.9	23
5	Porphyrin covalent organic nanodisks synthesized using acid-assisted exfoliation for improved bactericidal efficacy. Nanoscale Advances, 2022, 4, 2992-2995.	4.6	1
6	Femtosecond time-resolved diffuse reflectance study on facet engineered charge arrier dynamics in Ag3PO4 for antibiotics photodegradation. Applied Catalysis B: Environmental, 2021, 281, 119479.	20.2	42
7	Defect-mediated electron transfer in photocatalysts. Chemical Communications, 2021, 57, 3532-3542.	4.1	19
8	Single-Molecule Study of Redox Reaction Kinetics by Observing Fluorescence Blinking. Accounts of Chemical Research, 2021, 54, 1001-1010.	15.6	14
9	Electronic and Structural Properties of 2,3â€Naphthalimide in Openâ€Shell Configurations Investigated by Pulse Radiolytic and Theoretical Approaches. ChemistrySelect, 2021, 6, 3331-3338.	1.5	1
10	Control of Triplet Blinking Using Cyclooctatetraene to Access the Dynamics of Biomolecules at the Singleâ€Molecule Level. Angewandte Chemie, 2021, 133, 13051-13058.	2.0	3
11	Control of Triplet Blinking Using Cyclooctatetraene to Access the Dynamics of Biomolecules at the Singleâ€Molecule Level. Angewandte Chemie - International Edition, 2021, 60, 12941-12948.	13.8	11
12	Stacked Thiazole Orange Dyes in DNA Capable of Switching Emissive Behavior in Response to Structural Transitions. ChemBioChem, 2021, 22, 2729-2735.	2.6	3
13	COF-based photocatalyst for energy and environment applications. Surfaces and Interfaces, 2021, 25, 101249.	3.0	14
14	A cyanine dye based supramolecular photosensitizer enabling visible-light-driven organic reaction in water. Chemical Communications, 2021, 57, 11217-11220.	4.1	12
15	One-Pot Synthesis of Long Rutile TiO <sub>2</sub> Nanorods and Their Photocatalytic Activity for O <sub>2</sub> Evolution: Comparison with Near-Spherical Nanoparticles. ACS Omega, 2021, 6, 31557-31565.	3.5	6
16	Ultrathin ZnIn2S4 nanosheets with active (110) facet exposure and efficient charge separation for cocatalyst free photocatalytic hydrogen evolution. Applied Catalysis B: Environmental, 2020, 265, 118616.	20.2	132
17	Near Bandgap Excitation Inhibits the Interfacial Electron Transfer of Semiconductor/Cocatalyst. ACS Applied Materials & Interfaces, 2020, 12, 5920-5924.	8.0	23
18	Exfoliated Mo2C nanosheets hybridized on CdS with fast electron transfer for efficient photocatalytic H2 production under visible light irradiation. Applied Catalysis B: Environmental, 2020, 264, 118541.	20.2	79

#	Article	IF	CITATIONS
19	Visible light-driven photocatalytic duet reaction catalyzed by the B12-rhodium-titanium oxide hybrid catalyst. Journal of Organometallic Chemistry, 2020, 907, 121058.	1.8	12
20	Aggregation-induced photocatalytic activity and efficient photocatalytic hydrogen evolution of amphiphilic rhodamines in water. Chemical Science, 2020, 11, 11843-11848.	7.4	19
21	The formation mechanism of ZnTPyP fibers fabricated by a surfactant-assisted method. New Journal of Chemistry, 2020, 44, 13824-13833.	2.8	4
22	Synthesis of a B <sub>12</sub> –BODIPY dyad for B <sub>12</sub> -inspired photochemical transformations of a trichloromethylated organic compound. Chemical Communications, 2020, 56, 11945-11948.	4.1	9
23	Dynamics of Singleâ€Stranded RNA Looping Probed and Photoregulated by Sulfonated Pyrene. ChemistrySelect, 2020, 5, 8002-8008.	1.5	2
24	Inert basal plane activation of two-dimensional ZnIn <sub>2</sub> S <sub>4</sub> <i>via</i> Ni atom doping for enhanced co-catalyst free photocatalytic hydrogen evolution. Journal of Materials Chemistry A, 2020, 8, 13376-13384.	10.3	79
25	Hard X-ray excited optical luminescence from protein-directed Auâ^¼20 clusters. RSC Advances, 2020, 10, 13824-13829.	3.6	3
26	Shallow trap state-enhanced photocatalytic hydrogen evolution over thermal-decomposed polymeric carbon nitride. Chemical Communications, 2020, 56, 5921-5924.	4.1	18
27	Effect of Organic Additives during Hydrothermal Syntheses of Rutile TiO <sub>2</sub> Nanorods for Photocatalytic Applications. ACS Applied Nano Materials, 2019, 2, 5890-5899.	5.0	18
28	Shallow Trap State-Induced Efficient Electron Transfer at the Interface of Heterojunction Photocatalysts: The Crucial Role of Vacancy Defects. ACS Applied Materials & Interfaces, 2019, 11, 40860-40867.	8.0	63
29	The role of nitrogen defects in graphitic carbon nitride for visible-light-driven hydrogen evolution. Physical Chemistry Chemical Physics, 2019, 21, 2318-2324.	2.8	90
30	Monitoring Transport Behavior of Charge Carriers in a Single CdS@CuS Nanowire via In Situ Single-Particle Photoluminescence Spectroscopy. Journal of Physical Chemistry Letters, 2019, 10, 4017-4024.	4.6	37
31	Size-Dependent Relaxation Processes of Photoexcited [ <i>n</i> ]Cycloparaphenylenes ( <i>n</i> = 5–12): Significant Contribution of Internal Conversion in Smaller Rings. Journal of Physical Chemistry A, 2019, 123, 4737-4742.	2.5	19
32	Dual function of graphene oxide for assisted exfoliation of black phosphorus and electron shuttle in promoting visible and near-infrared photocatalytic H2 evolution. Applied Catalysis B: Environmental, 2019, 256, 117864.	20.2	41
33	In situ observation of NiS nanoparticles depositing on single TiO2 mesocrystal for enhanced photocatalytic hydrogen evolution activity. Applied Catalysis B: Environmental, 2019, 254, 594-600.	20.2	50
34	Charge-Separated Mixed Valency in an Unsymmetrical Acceptor–Donor–Donor Triad Based on Diarylboryl and Triarylamine Units. Journal of Organic Chemistry, 2019, 84, 8910-8920.	3.2	14
35	Ultrafast spectroscopic study of plasmon-induced hot electron transfer under NIR excitation in Au triangular nanoprism/g-C <sub>3</sub> N <sub>4</sub> for photocatalytic H <sub>2</sub> production. Chemical Communications, 2019, 55, 6014-6017.	4.1	45
36	Formation of the Chargeâ€Localized Dimer Radical Cation of 2â€Ethylâ€9,10â€dimethoxyanthracene in Solution Phase. Chemistry - A European Journal, 2019, 25, 5586-5594.	3.3	2

#	Article	IF	CITATIONS
37	Black Phosphorus Sensitized TiO <sub>2</sub> Mesocrystal Photocatalyst for Hydrogen Evolution with Visible and Near-Infrared Light Irradiation. ACS Catalysis, 2019, 9, 3618-3626.	11.2	115
38	Proton Transfer Accompanied by the Oxidation of Adenosine. Chemistry - A European Journal, 2019, 25, 7711-7718.	3.3	6
39	Unprecedented effect of CO2 calcination atmosphere on photocatalytic H2 production activity from water using g-C3N4 synthesized from triazole polymerization. Applied Catalysis B: Environmental, 2019, 241, 141-148.	20.2	62
40	Innentitelbild: Zâ€Scheme Photocatalytic Water Splitting on a 2D Heterostructure of Black Phosphorus/Bismuth Vanadate Using Visible Light (Angew. Chem. 8/2018). Angewandte Chemie, 2018, 130, 2026-2026.	2.0	1
41	Faster Electron Injection and More Active Sites for Efficient Photocatalytic H <sub>2</sub> Evolution in gâ€C <sub>3</sub> N <sub>4</sub> /MoS <sub>2</sub> Hybrid. Small, 2018, 14, e1703277.	10.0	206
42	Anisotropic Ag <sub>2</sub> S–Au Triangular Nanoprisms with Desired Configuration for Plasmonic Photocatalytic Hydrogen Generation in Visible/Nearâ€Infrared Region. Advanced Functional Materials, 2018, 28, 1706969.	14.9	54
43	Reaction dynamics of excited radical ions revealed by femtosecond laser flash photolysis. Journal of Photochemistry and Photobiology C: Photochemistry Reviews, 2018, 35, 25-37.	11.6	31
44	Z‣cheme Photocatalytic Water Splitting on a 2D Heterostructure of Black Phosphorus/Bismuth Vanadate Using Visible Light. Angewandte Chemie - International Edition, 2018, 57, 2160-2164.	13.8	506
45	Excited-State Properties of Radical Anions of C70 and Its Derivatives: Significant Differences from the Case of C60. Journal of Physical Chemistry C, 2018, 122, 13385-13390.	3.1	5
46	Zâ€Scheme Photocatalytic Water Splitting on a 2D Heterostructure of Black Phosphorus/Bismuth Vanadate Using Visible Light. Angewandte Chemie, 2018, 130, 2182-2186.	2.0	356
47	The Development of Functional Mesocrystals for Energy Harvesting, Storage, and Conversion. Chemistry - A European Journal, 2018, 24, 6295-6307.	3.3	26
48	Noble metal-free near-infrared-driven photocatalyst for hydrogen production based on 2D hybrid of black Phosphorus/WS2. Applied Catalysis B: Environmental, 2018, 221, 645-651.	20.2	171
49	Aggregationâ€Induced Singlet Oxygen Generation: Functional Fluorophore and Anthrylphenylene Dyad Selfâ€Assemblies. Chemistry - A European Journal, 2018, 24, 636-645.	3.3	29
50	Au Nanorod Photosensitized La <sub>2</sub> Ti <sub>2</sub> O <sub>7</sub> Nanosteps: Successive Surface Heterojunctions Boosting Visible to Near-Infrared Photocatalytic H <sub>2</sub> Evolution. ACS Catalysis, 2018, 8, 122-131.	11.2	114
51	Significant structural relaxations of excited [ <i>n</i> ]cycloparaphenylene dications ( <i>n</i> = 5–9). Physical Chemistry Chemical Physics, 2018, 20, 29207-29211.	2.8	5
52	Influence of Charge Distribution on Structural Changes of Aromatic Imide Derivatives upon One-Electron Reduction Revealed by Time-Resolved Resonance Raman Spectroscopy during Pulse Radiolysis. Journal of Physical Chemistry A, 2018, 122, 8738-8744.	2.5	8
53	2D/2D Heterostructured CdS/WS <sub>2</sub> with Efficient Charge Separation Improving H <sub>2</sub> Evolution under Visible Light Irradiation. ACS Applied Materials & Interfaces, 2018, 10, 20458-20466.	8.0	137
54	Defect state-induced efficient hot electron transfer in Au nanoparticles/reduced TiO <sub>2</sub> mesocrystal photocatalysts. Chemical Communications, 2018, 54, 6052-6055.	4.1	43

#	Article	IF	CITATIONS
55	Pulse Radiolysis of TIPS-Pentacene and a Fluorene-bridged Bis(pentacene): Evidence for Intramolecular Singlet-Exciton Fission. Journal of Physical Chemistry Letters, 2018, 9, 3934-3938.	4.6	12
56	Facet Effects of Ag <sub>3</sub> PO <sub>4</sub> on Chargeâ€Carrier Dynamics: Tradeâ€Off Between Photocatalytic Activity and Chargeâ€Carrier Lifetime. Chemistry - A European Journal, 2018, 24, 14928-14932.	3.3	18
57	Defects rich g-C3N4 with mesoporous structure for efficient photocatalytic H2 production under visible light irradiation. Applied Catalysis B: Environmental, 2018, 238, 638-646.	20.2	169
58	Spirally Configured ( <i>cis</i> -Stilbene) Trimers: Steady-State and Time-Resolved Photophysical Studies and Organic Light-Emitting Diode Applications. ACS Applied Materials & Interfaces, 2018, 10, 25561-25569.	8.0	4
59	Factors affecting photocatalytic activity of visible light-responsive titanium dioxide doped with chromium ions. Catalysis Science and Technology, 2018, 8, 4726-4733.	4.1	7
60	Charge Carrier Dynamics in TiO <sub>2</sub> Mesocrystals with Oxygen Vacancies for Photocatalytic Hydrogen Generation under Solar Light Irradiation. Journal of Physical Chemistry C, 2018, 122, 15163-15170.	3.1	43
61	Amplifying fluorescence signal contrast of aptamer-modified microspheres inspired by whispering-gallery mode lasing. RSC Advances, 2018, 8, 20822-20828.	3.6	0
62	Au/La <sub>2</sub> Ti <sub>2</sub> O <sub>7</sub> Nanostructures Sensitized with Black Phosphorus for Plasmonâ€Enhanced Photocatalytic Hydrogen Production in Visible and Nearâ€Infrared Light. Angewandte Chemie - International Edition, 2017, 56, 2064-2068.	13.8	284
63	Au/La <sub>2</sub> Ti <sub>2</sub> O <sub>7</sub> Nanostructures Sensitized with Black Phosphorus for Plasmonâ€Enhanced Photocatalytic Hydrogen Production in Visible and Nearâ€Infrared Light. Angewandte Chemie, 2017, 129, 2096-2100.	2.0	51
64	TiO2 mesocrystals composited with gold nanorods for highly efficient visible-NIR-photocatalytic hydrogen production. Nano Energy, 2017, 35, 1-8.	16.0	95
65	Two-Dimensional Au-Nanoprism/Reduced Graphene Oxide/Pt-Nanoframe as Plasmonic Photocatalysts with Multiplasmon Modes Boosting Hot Electron Transfer for Hydrogen Generation. Journal of Physical Chemistry Letters, 2017, 8, 844-849.	4.6	61
66	Dual Character of Excited Radical Anions in Aromatic Diimide Bis(radical anion)s: Donor or Acceptor?. Journal of Physical Chemistry C, 2017, 121, 4558-4563.	3.1	28
67	In situ nitrogen-doped hollow-TiO <sub>2</sub> /g-C <sub>3</sub> N <sub>4</sub> composite photocatalysts with efficient charge separation boosting water reduction under visible light. Journal of Materials Chemistry A, 2017, 5, 9671-9681.	10.3	118
68	Charge separation in a nanostep structured perovskite-type photocatalyst induced by successive surface heterojunctions. Journal of Materials Chemistry A, 2017, 5, 10442-10449.	10.3	34
69	Radical Ions of a π-Bowl Sumanene: Effects of Strained Structure on the Electronic Transitions. Journal of Physical Chemistry A, 2017, 121, 4902-4906.	2.5	2
70	Black phosphorus: A promising two dimensional visible and near-infrared-activated photocatalyst for hydrogen evolution. Applied Catalysis B: Environmental, 2017, 217, 285-292.	20.2	164
71	Topotactic Epitaxy of SrTiO <sub>3</sub> Mesocrystal Superstructures with Anisotropic Construction for Efficient Overall Water Splitting. Angewandte Chemie, 2017, 129, 5383-5387.	2.0	14
72	Topotactic Epitaxy of SrTiO <sub>3</sub> Mesocrystal Superstructures with Anisotropic Construction for Efficient Overall Water Splitting. Angewandte Chemie - International Edition, 2017, 56, 5299-5303.	13.8	92

#	Article	IF	CITATIONS
73	Eco-Friendly Photochemical Production of H <sub>2</sub> O <sub>2</sub> through O <sub>2</sub> Reduction over Carbon Nitride Frameworks Incorporated with Multiple Heteroelements. ACS Catalysis, 2017, 7, 2886-2895.	11.2	287
74	Photoaccelerated Hole Transfer in Oligothiophene Assemblies. Journal of Physical Chemistry C, 2017, 121, 649-655.	3.1	6
75	<i>In Situ</i> Observation of Single Au Triangular Nanoprism Etching to Various Shapes for Plasmonic Photocatalytic Hydrogen Generation. ACS Nano, 2017, 11, 968-974.	14.6	63
76	Hot electron-driven hydrogen evolution using anisotropic gold nanostructure assembled monolayer MoS <sub>2</sub> . Nanoscale, 2017, 9, 1520-1526.	5.6	55
77	Charge transfer dynamics in DNA revealed by time-resolved spectroscopy. Chemical Science, 2017, 8, 1752-1762.	7.4	29
78	Phase Effect of Ni <sub><i>x</i></sub> P <sub><i>y</i></sub> Hybridized with g-C <sub>3</sub> N <sub>4</sub> for Photocatalytic Hydrogen Generation. ACS Applied Materials & Interfaces, 2017, 9, 30583-30590.	8.0	116
79	Metal-Free Photocatalyst for H <sub>2</sub> Evolution in Visible to Near-Infrared Region: Black Phosphorus/Graphitic Carbon Nitride. Journal of the American Chemical Society, 2017, 139, 13234-13242.	13.7	907
80	g-C <sub>3</sub> N <sub>4</sub> /TiO <sub>2</sub> Mesocrystals Composite for H <sub>2</sub> Evolution under Visible-Light Irradiation and Its Charge Carrier Dynamics. ACS Applied Materials & Interfaces, 2017, 9, 34844-34854.	8.0	163
81	Live Cell Imaging Using Photoswitchable Diaryletheneâ€Doped Fluorescent Polymer Dots. Chemistry - an Asian Journal, 2017, 12, 2660-2665.	3.3	14
82	Graphitic-C3N4 hybridized N-doped La2Ti2O7 two-dimensional layered composites as efficient visible-light-driven photocatalyst. Applied Catalysis B: Environmental, 2017, 202, 191-198.	20.2	107
83	6 Radiation Chemical Studies on Reaction Mechanisms. Radioisotopes, 2017, 66, 437-449.	0.2	Ο
84	Sequenceâ€Dependent Photocurrent Generation through Longâ€Distance Excessâ€Electron Transfer in DNA. Angewandte Chemie, 2016, 128, 8857-8859.	2.0	4
85	Sequenceâ€Dependent Photocurrent Generation through Longâ€Distance Excessâ€Electron Transfer in DNA. Angewandte Chemie - International Edition, 2016, 55, 8715-8717.	13.8	11
86	Structures of 4-substituted thioanisole radical cations studied by time-resolved resonance Raman spectroscopy during pulse radiolysis and theoretical calculations. RSC Advances, 2016, 6, 109334-109339.	3.6	4
87	Singlet–singlet and singlet–triplet annihilations in structure-regulated porphyrin polymers. Journal of Photochemistry and Photobiology A: Chemistry, 2016, 331, 56-59.	3.9	8
88	Pt–Au Triangular Nanoprisms with Strong Dipole Plasmon Resonance for Hydrogen Generation Studied by Single-Particle Spectroscopy. ACS Nano, 2016, 10, 6299-6305.	14.6	151
89	Development of tailored TiO2 mesocrystals for solar driven photocatalysis. Journal of Energy Chemistry, 2016, 25, 917-926.	12.9	30
90	Unprecedented Intramolecular Electron Transfer from Excited Perylenediimide Radical Anion. Journal of Physical Chemistry C, 2016, 120, 12734-12741.	3.1	45

#	Article	IF	CITATIONS
91	Excess-Electron Transfer in DNA by a Fluctuation-Assisted Hopping Mechanism. Journal of Physical Chemistry B, 2016, 120, 660-666.	2.6	11
92	Atomic Layer Deposition-Confined Nonstoichiometric TiO <sub>2</sub> Nanocrystals with Tunneling Effects for Solar Driven Hydrogen Evolution. Journal of Physical Chemistry Letters, 2016, 7, 1173-1179.	4.6	18
93	Excited-state dynamics of Si–rhodamine and its aggregates: versatile fluorophores for NIR absorption. Physical Chemistry Chemical Physics, 2016, 18, 2097-2103.	2.8	8
94	Covalently Attached Porphycene–Ferrocene Dyads: Synthesis, Redox-Switched Emission, and Observation of the Charge-Separated State. Inorganic Chemistry, 2016, 55, 7-9.	4.0	9
95	Dynamics of Excess-Electron Transfer through Alternating Adenine:Thymine Sequences in DNA. Chemistry - A European Journal, 2015, 21, 16190-16194.	3.3	7
96	Photoinduced Electron Transfer of Porphyrin Isomers: Impact of Molecular Structures on Electronâ€Transfer Dynamics. Chemistry - an Asian Journal, 2015, 10, 2320-2326.	3.3	4
97	The unprecedented J-aggregate formation of rhodamine moieties induced by 9-phenylanthracenyl substitution. Chemical Communications, 2015, 51, 11580-11583.	4.1	27
98	Proton Transfer of Guanine Radical Cations Studied by Time-Resolved Resonance Raman Spectroscopy Combined with Pulse Radiolysis. Journal of Physical Chemistry Letters, 2015, 6, 5045-5050.	4.6	27
99	Dual electron transfer pathways from the excited C60 radical anion: enhanced reactivities due to the photoexcitation of reaction intermediates. Physical Chemistry Chemical Physics, 2015, 17, 31030-31038.	2.8	12
100	Configurational changes of heme followed by cytochrome c folding reaction. Molecular BioSystems, 2015, 11, 218-222.	2.9	7
101	Structural Study of Various Substituted Biphenyls and Their Radical Anions Based on Time-Resolved Resonance Raman Spectroscopy Combined with Pulse Radiolysis. Journal of Physical Chemistry A, 2015, 119, 851-856.	2.5	20
102	Efficient charge separation on 3D architectures of TiO <sub>2</sub> mesocrystals packed with a chemically exfoliated MoS <sub>2</sub> shell in synergetic hydrogen evolution. Chemical Communications, 2015, 51, 7187-7190.	4.1	76
103	Detection of Structural Changes upon One-Electron Oxidation and Reduction of Stilbene Derivatives by Time-Resolved Resonance Raman Spectroscopy during Pulse Radiolysis and Theoretical Calculations. Journal of Physical Chemistry A, 2015, 119, 6816-6822.	2.5	11
104	How Does Guanine–Cytosine Base Pair Affect Excess-Electron Transfer in DNA?. Journal of Physical Chemistry B, 2015, 119, 7994-8000.	2.6	17
105	Radical Ions of Cyclopyrenylene: Comparison of Spectral Properties with Cycloparaphenylene. Journal of Physical Chemistry A, 2015, 119, 4136-4141.	2.5	8
106	Intermolecular and Intramolecular Electron Transfer Processes from Excited Naphthalene Diimide Radical Anions. Journal of Physical Chemistry B, 2015, 119, 7275-7282.	2.6	52
107	A nanocomposite superstructure of metal oxides with effective charge transfer interfaces. Nature Communications, 2014, 5, 3038.	12.8	128
108	Au/TiO <sub>2</sub> Superstructure-Based Plasmonic Photocatalysts Exhibiting Efficient Charge Separation and Unprecedented Activity. Journal of the American Chemical Society, 2014, 136, 458-465.	13.7	651

#	Article	IF	CITATIONS
109	Driving Force Dependence of Charge Separation and Recombination Processes in Dyads of Nucleotides and Strongly Electron-Donating Oligothiophenes. Journal of Physical Chemistry B, 2014, 118, 12186-12191.	2.6	9
110	Radical Ions of Cycloparaphenylenes: Size Dependence Contrary to the Neutral Molecules. Journal of Physical Chemistry Letters, 2014, 5, 2302-2305.	4.6	48
111	Radical Cation of Star-Shaped Condensed Oligofluorenes Having Isotruxene as a Core: Importance of Rigid Planar Structure on Charge Delocalization. Journal of Physical Chemistry A, 2014, 118, 2307-2315.	2.5	17
112	Far-Red Fluorescence Probe for Monitoring Singlet Oxygen during Photodynamic Therapy. Journal of the American Chemical Society, 2014, 136, 11707-11715.	13.7	229
113	Properties of Triplet-Excited [ <i>n</i> ]Cycloparaphenylenes ( <i>n</i> = 8–12): Excitation Energies Lower than Those of Linear Oligomers and Polymers. Journal of Physical Chemistry A, 2014, 118, 4527-4532.	2.5	56
114	Solvent Dynamics Regulated Electron Transfer in S <sub>2</sub> -Excited Sb and Ge Tetraphenylporphyrins with an Electron Donor Substituent at the Meso-Position. Journal of Physical Chemistry A, 2014, 118, 3926-3933.	2.5	8
115	Fundamental Reaction Mechanisms in Radiation Chemistry and Recent Examples. , 2014, , 3-32.		0
116	Synthesis and physical properties of a ball-like three-dimensional π-conjugated molecule. Nature Communications, 2013, 4, 2694.	12.8	139
117	Photoinduced electron transfer in supramolecular donor–acceptor dyads of Zn corrphycene. Physical Chemistry Chemical Physics, 2013, 15, 5677.	2.8	7
118	Photodissociation of pyrene dimer radical cation during the pulse radiolysis–laser flash photolysis combined method. Research on Chemical Intermediates, 2013, 39, 449-461.	2.7	11
119	Î <sup>3</sup> -Ray radiolysis and theoretical study on radical ions of star-shaped oligofluorenes having a truxene or isotruxene as a core. Chemical Physics, 2013, 419, 118-123.	1.9	7
120	Efficient Electron Transfer in iâ€Motif DNA with a Tetraplex Structure. Angewandte Chemie - International Edition, 2013, 52, 12937-12941.	13.8	15
121	Enhancement of the Quinoidal Character for Smaller [ <i>n</i> ]Cycloparaphenylenes Probed by Raman Spectroscopy. ChemPhysChem, 2013, 14, 1570-1572.	2.1	49
122	Size-dependent fluorescence properties of [n]cycloparaphenylenes (n = 8–13), hoop-shaped Ĩ€-conjugated molecules. Physical Chemistry Chemical Physics, 2012, 14, 14585.	2.8	150
123	Excess electron transfer dynamics in DNA hairpins conjugated with N,N-dimethylaminopyrene as a photosensitizing electron donor. Chemical Communications, 2012, 48, 11008.	4.1	16
124	Folding Dynamics of Cytochrome <i>c</i> Using Pulse Radiolysis. Journal of the American Chemical Society, 2012, 134, 13430-13435.	13.7	12
125	Hole and excess electron transfer dynamics in DNA. Physical Chemistry Chemical Physics, 2012, 14, 11234.	2.8	43
126	Excessâ€Electron Injection and Transfer in Terthiopheneâ€Modified DNA: Terthiophene as a Photosensitizing Electron Donor for Thymine, Cytosine, and Adenine. Chemistry - A European Journal, 2012, 18, 2056-2062.	3.3	18

#	Article	IF	CITATIONS
127	Direct Measurement of the Dynamics of Excess Electron Transfer through Consecutive Thymine Sequence in DNA. Journal of the American Chemical Society, 2011, 133, 15320-15323.	13.7	66
128	Delocalization of Positive Charge in π-Stacked Multi-benzene Rings in Multilayered Cyclophanes. Journal of Physical Chemistry A, 2011, 115, 741-746.	2.5	30
129	Structural Relaxation in the Singlet Excited State of Star-Shaped Oligofluorenes Having a Truxene or Isotruxene as a Core. Journal of Physical Chemistry B, 2011, 115, 13502-13507.	2.6	14
130	Recent Approach in Radiation Chemistry toward Material and Biological Science. Journal of Physical Chemistry Letters, 2011, 2, 2965-2971.	4.6	23
131	Reorganization energy of supramolecular donor–acceptor dyad of octaethylporphyrin isomers and axial-coordinated acceptor: Experimental and computational study. Journal of Photochemistry and Photobiology A: Chemistry, 2011, 217, 242-248.	3.9	10
132	Sequence Dependence of Excess Electron Transfer in DNAâ€. Journal of Physical Chemistry B, 2010, 114, 14657-14663.	2.6	40
133	Electron Transfer in the Supramolecular Donorâ ``Acceptor Dyad of Zinc Hemiporphycene. Journal of Physical Chemistry A, 2010, 114, 4156-4162.	2.5	10
134	Electron Transfer from Oligothiophenes in the Higher Triplet Excited States. Journal of Physical Chemistry A, 2010, 114, 10789-10794.	2.5	6
135	Synthesis of a Novel Sn(IV) Porphyceneâ^'Ferrocene Triad Linked by Axial Coordination and Solvent Polarity Effect in Photoinduced Charge Separation Process. Inorganic Chemistry, 2010, 49, 2872-2880.	4.0	21
136	Electron Transfer in the Supramolecular Donorâ^'Acceptor Dyad of Zinc Porphycene. Journal of Physical Chemistry A, 2009, 113, 3330-3335.	2.5	22
137	"Signal-On―Detection of DNA Hole Transfer at the Single Molecule Level. Journal of the American Chemical Society, 2009, 131, 6656-6657.	13.7	22
138	Emission Mechanism of Doubly ortho-Linked Quinoxaline/Diphenylfluorene or cis-Stilbene/Fluorene Hybrid Compounds Based on the Transient Absorption and Emission Measurements during Pulse Radiolysis. Journal of the American Chemical Society, 2009, 131, 6698-6707.	13.7	35
139	Intramolecular dimer radical anions of [3n] cyclophanes: transannular distance dependent stabilization energy. Chemical Communications, 2009, , 1553.	4.1	21
140	Photocatalytic Cleavage of Single TiO <sub>2</sub> /DNA Nanoconjugates. Chemistry - A European Journal, 2008, 14, 1492-1498.	3.3	29
141	Two‣aserâ€Guided Threeâ€Dimensional Microfabrication and Processing in a Flexible Polymer Matrix. Advanced Materials, 2008, 20, 3427-3432.	21.0	20
142	Three-Dimensional Writing of Copper Nanoparticles in a Polymer Matrix with Two-Color Laser Beams. Chemistry of Materials, 2008, 20, 2060-2062.	6.7	24
143	Properties of Excited Radical Cations of Substituted Oligothiophenes. Journal of Physical Chemistry A, 2008, 112, 11312-11318.	2.5	11
144	Excitation Energy Dependence of Photoinduced Processes in Pentathiopheneâ^'Perylene Bisimide Dyads with a Flexible Linker. Journal of Physical Chemistry A, 2008, 112, 10193-10199.	2.5	30

#	Article	IF	CITATIONS
145	Kinetics of charge transfer in DNA containing a mismatch. Nucleic Acids Research, 2008, 36, 5562-5570.	14.5	42
146	Single-molecule observation of DNA charge transfer. Proceedings of the National Academy of Sciences of the United States of America, 2007, 104, 11179-11183.	7.1	59
147	Electron Transfer from the S1and S2States of Pentacoordinated Tetrapyrrole Macrocycles to Pyromellitic Diimide as an Axial Ligand. Journal of Physical Chemistry A, 2007, 111, 11430-11436.	2.5	23
148	Intermolecular Electron Transfer from Excited Benzophenone Ketyl Radical. Journal of Physical Chemistry A, 2007, 111, 223-229.	2.5	27
149	Design of Cyclic Reaction Driven by Two-Color Two-Photon Excitation. Journal of Physical Chemistry C, 2007, 111, 6917-6919.	3.1	8
150	Energy Levels of Oligothiophenes in the Higher Excited Triplet States. Journal of Physical Chemistry C, 2007, 111, 1024-1028.	3.1	10
151	Electron Transfer from Axial Ligand to S1- and S2-Excited Phosphorus Tetraphenylporphyrin. Journal of Physical Chemistry A, 2007, 111, 10574-10579.	2.5	65
152	Bimolecular Hole Transfer from the Trimethoxybenzene Radical Cation in the Excited State. Journal of Physical Chemistry A, 2007, 111, 4743-4747.	2.5	7
153	Intramolecular Triplet Energy Transfer via Higher Triplet Excited State during Stepwise Two-Color Two-Laser Irradiation. Journal of Physical Chemistry A, 2007, 111, 9781-9788.	2.5	13
154	Properties and Reactivity of Xanthyl Radical in the Excited State. Journal of Physical Chemistry A, 2006, 110, 9788-9792.	2.5	4
155	Intramolecular Electron Transfer from Axial Ligand to S2-Excited Sb-Tetraphenylporphyrin. Journal of Physical Chemistry B, 2006, 110, 9368-9370.	2.6	21
156	Rapid Long-Distance Hole Transfer through Consecutive Adenine Sequence. Journal of the American Chemical Society, 2006, 128, 11012-11013.	13.7	52
157	Solvent Effect on the Deactivation Processes of Benzophenone Ketyl Radicals in the Excited State. Journal of Physical Chemistry A, 2006, 110, 11800-11808.	2.5	17
158	Transannular Distance Dependence of Stabilization Energy of the Intramolecular Dimer Radical Cation of Cyclophanes. Journal of Physical Chemistry A, 2006, 110, 5735-5739.	2.5	26
159	Photodissociation of Naphthalene Dimer Radical Cation during the Two-Color Two-Laser Flash Photolysis and Pulse Radiolysisâ^'Laser Flash Photolysis. Journal of Physical Chemistry A, 2006, 110, 9319-9324.	2.5	24
160	Formation of Pyrene Dimer Radical Cation at the Minor Groove of DNA. Bulletin of the Chemical Society of Japan, 2006, 79, 312-316.	3.2	5
161	Two-color two-laser fabrication of gold nanoparticles in a PVA film. Chemical Physics Letters, 2006, 420, 90-94.	2.6	46
162	Direct fluorescence lifetime measurement of excited radical cation of 1,3,5-trimethoxybenzene by ns–ps two-color two-laser flash photolysis. Chemical Physics Letters, 2006, 432, 436-440.	2.6	8

#	Article	IF	CITATIONS
163	Properties of Excited Ketyl Radicals of Benzophenone Analogues Affected by the Size and Electronic Character of the Aromatic Ring Systems. Chemistry - A European Journal, 2006, 12, 1610-1617.	3.3	14
164	Charge transfer through DNA nanoscaled assembly programmable with DNA building blocks. Proceedings of the National Academy of Sciences of the United States of America, 2006, 103, 18072-18076.	7.1	65
165	Contributions of the Distance-Dependent Reorganization Energy and Proton-Transfer to the Hole-Transfer Process in DNA. Chemistry - A European Journal, 2005, 11, 3835-3842.	3.3	83
166	Synthesis and properties of terthiophene-modified oligodeoxynucleotides. Bioorganic and Medicinal Chemistry Letters, 2005, 15, 4547-4549.	2.2	8
167	Photophysical Properties of Oligo(2,3-Thienyleneethynylene)s. Journal of Physical Chemistry B, 2005, 109, 10695-10698.	2.6	7
168	Remarkable Reactivities of the Xanthone Ketyl Radical in the Excited State Compared with That in the Ground State. Journal of Physical Chemistry A, 2005, 109, 2452-2458.	2.5	13
169	Formation of Highly Stabilized Intramolecular Dimer Radical Cation and π-Complex of [3n]Cyclophanes (n= 3, 5, 6) during Pulse Radiolysis. Journal of Physical Chemistry A, 2005, 109, 3531-3534.	2.5	21
170	Importance of Properties of the Lowest and Higher Singlet Excited States on the Resonant Two-Photon Ionization of Stilbene and Substituted Stilbenes Using Two-Color Two-Lasers. Journal of Physical Chemistry A, 2005, 109, 9831-9835.	2.5	16
171	Dual Electron Transfer Pathways from 4,4â€~-Dimethoxybenzophenone Ketyl Radical in the Excited State to Parent Molecule in the Ground State. Journal of Physical Chemistry A, 2005, 109, 6830-6835.	2.5	14
172	Fast Exciton Migration in Porphyrin-Functionalized Polypeptides. Journal of Physical Chemistry B, 2005, 109, 33-35.	2.6	38
173	Kinetics of Transient End-to-End Contact of Single-Stranded DNAs. Journal of the American Chemical Society, 2005, 127, 13232-13237.	13.7	23
174	Ultrafast Photoinduced Intramolecular Charge Separation and Recombination Processes in the Oligothiophene-Substituted Benzene Dyads with an Amide Spacer. Journal of Physical Chemistry B, 2005, 109, 19257-19262.	2.6	16
175	Anomalous Fluorescence from the Azaxanthone Ketyl Radical in the Excited State. Journal of the American Chemical Society, 2005, 127, 3702-3703.	13.7	23
176	First Direct Observation of the Higher Triplet Excited States of Substituted Oligothiophenes by Two-Color Two-Laser Flash Photolysis. ChemPhysChem, 2004, 5, 1240-1242.	2.1	13
177	Direct observation of hole transfer through double-helical DNA over 100 A. Proceedings of the National Academy of Sciences of the United States of America, 2004, 101, 14002-14006.	7.1	156
178	Rapid Exciton Migration and Fluorescent Energy Transfer in Helical Polyisocyanides with Regularly Arranged Porphyrin Pendants. Journal of Physical Chemistry B, 2004, 108, 11935-11941.	2.6	65
179	Charge Separation in DNA via Consecutive Adenine Hopping. Journal of the American Chemical Society, 2004, 126, 1125-1129.	13.7	146
180	Transient Absorption Spectra and Lifetimes of Benzophenone Ketyl Radicals in the Excited State. Journal of Physical Chemistry A, 2004, 108, 8147-8150.	2.5	45

#	Article	IF	CITATIONS
181	Higher Triplet Excited States of Oligo(p-phenylenevinylene)s. Journal of Physical Chemistry B, 2004, 108, 16727-16731.	2.6	12
182	Competitive Marcus-Type Electron Transfer and Energy Transfer from the Higher Triplet Excited State. Journal of Physical Chemistry A, 2004, 108, 10941-10948.	2.5	10
183	Intermolecular Electron Transfer from Naphthalene Derivatives in the Higher Triplet Excited States. Journal of the American Chemical Society, 2004, 126, 9709-9714.	13.7	30
184	Improvement of Quantum Yields for Photoinduced Energy/Electron Transfer by Isolation of Self-Aggregative Zinc Tetraphenyl Porphyrin-Pendant Polymer Using Cyclodextrin Inclusion in Aqueous Solution. Journal of Physical Chemistry B, 2003, 107, 11261-11266.	2.6	66
185	Small Reorganization Energy of Intramolecular Electron Transfer in Fullerene-Based Dyads with Short Linkage. Journal of Physical Chemistry A, 2002, 106, 10991-10998.	2.5	87
186	Spectroscopic, Electrochemical, and Photochemical Studies of Self-Assembled via Axial Coordination Zinc Porphyrinâ^Fulleropyrrolidine Dyads. Journal of Physical Chemistry A, 2002, 106, 3243-3252.	2.5	238
187	Photoinduced Charge Separation and Recombination Processes in Fine Particles of Oligothiophene-C60Dyad Molecules. Journal of Physical Chemistry B, 2001, 105, 9930-9934.	2.6	67
188	Pico- and nano-second laser flash photolysis study on photoinduced charge separation in oligothiophene-C60 dyad molecules. Research on Chemical Intermediates, 2001, 27, 73-88.	2.7	56
189	Photoinduced Electron Transfer from Oligothiophenes/Polythiophene to Fullerenes (C60/C70) in Solution:  Comprehensive Study by Nanosecond Laser Flash Photolysis Method. Journal of Physical Chemistry B, 2000, 104, 11632-11638.	2.6	110
190	Solvent Polarity Dependence of Photoinduced Charge Separation in a Tetrathiophene-C60Dyad Studied by Pico- and Nanosecond Laser Flash Photolysis in the Near-IR Region. Journal of Physical Chemistry A, 2000, 104, 4876-4881.	2.5	145
191	Electron-Transfer Reactions between Fullerenes (C60and C70) and Tetrakis(dimethylamino)ethylene in the Ground and Excited States. Journal of Physical Chemistry B, 1999, 103, 445-449.	2.6	46
192	Enhanced Reactivity of C70in the Photochemical Reactions with NADH and NAD Dimer Analogues As Compared to C60via Photoinduced Electron Transfer. Journal of Physical Chemistry A, 1999, 103, 5935-5941.	2.5	30
193	Photophysical properties of bis(2,2′-bithiophene-5-yl)benzenes. Journal of the Chemical Society, Faraday Transactions, 1998, 94, 2355.	1.7	19
194	Selective One-Electron and Two-Electron Reduction of C60 with NADH and NAD Dimer Analogues via Photoinduced Electron Transfer. Journal of the American Chemical Society, 1998, 120, 8060-8068.	13.7	221
195	Photochemical Generation of Radical Cations of Dithienothiophenes, Condensed Thiophene Trimers, Studied by Laser Flash Photolysis. Journal of Physical Chemistry A, 1997, 101, 1056-1061.	2.5	25